

7-4 AMATERASU: Model for Atmospheric TeraHertz Radiation Analysis and Simulation

Philippe Baron, Jana Mendrok, KASAI Yasuko, OCHIAI Satoshi, SETA Takamasa, SAGI Kazutoshi, SUZUKI Kodai, SAGAWA Hideo, and Joachim Urban

We describe the current status of the Advanced Model for Atmospheric TeraHertz Radiation Analysis and SimUlation (AMATERASU) that is being developed in the framework of the NICT THz project. This code aims to be used for studying the interest of the THz frequency region for atmospheric remote sensing, communication systems and estimate the impact of the THz thermal atmospheric emission in the Earth energy budget. This paper presents the first stage of the model development that concerns a non scattering and a horizontal homogeneous atmosphere, e.g., the geophysical parameters are only altitude dependent. A scattering module is being developed but it is presented in an other paper in this issue. The model is based on the Microwave Observation and Lines Estimation and REtrieval code (MOLIERE). The absorption coefficient module has been modified in order to extend the frequency coverage from the sub-millimeter wavelength to the near InfraRed region. A new radiative transfer module has been implemented that can handle the different types of optical paths and any location for the receiver. AMATERASU includes the original MOLIERE instrument simulator and retrieval codes. The validation methodology is discussed and some examples of the current applications are given. The next steps of the development are presented in the conclusion including the modeling of the horizontal inhomogeneties in the atmopshere.

Keywords

AMATERASU, Radiative Transfer, Terahertz, Atmospheric propagation, Atmospheric remote sensing

1 Introduction

The observation of the Earth thermal emission spectrum provides relevant informations about the chemical composition, the temperature and the dynamics of the atmosphere as well as properties of the clouds. A special focus must be put on the free troposphere (above the boundary layer) and the lower stratosphere to understand 1) the climate and its future evolution, and 2) the impacts of the pollution and the biomass burning in the atmospheric composition:

- (1) The radiative emission in the THz spectral range of the upper troposphere due to water vapor (H₂O), ozone (O₃) and ice clouds, has a significant contribution in the Earth radiative budget^[1]. This contribution is still not well known because of the limitations of current instruments and the strong variability of the upper troposphere state^{[2]-[4]}.
- (2) The pollution and the biomass burning are important sources of chemical components in the atmosphere^[5]. Long lived species are produced at the surface and transported

to the free troposphere and lower stratosphere^{[6][7]}. The pollutants deteriorate the quality of the air and reduce its oxidation capacity.

So far, the nadir and limb space-borne sounders operate either in the region below the sub-millimeter wavelength^{[8]-[10]} or in the region above the far-IR (650 cm^{-1})^{[11][12]}. The THz spectral region between 100 and 500 cm^{-1} , also referred as the Far InfraRed region, has not been explored yet. It is characterized by strong changes in the atmospheric transmission, with windows that allows nadir sounding down to the lower troposphere. The spectrum of the atmospheric thermal emission is dominated by the strongest H₂O lines. Furthermore, THz observations will be less and differently sensitive to tropospheric clouds than the measurements at infrared wavelengths. Also, this region is rich of numerous lines of trace gases.

As demonstrated by the Far-Infrared Spectroscopy of the Troposphere (FIRST) instrument^[13], the new technology developments make possible to develop satellite sensors covering the full IR region including the THz region. Hence, the estimation of the capabilities of THz sounders becomes an interesting issue with the possibility of near future applications.

The Advanced Model for Atmospheric Terahertz Radiation Analysis and Simulation (AMATERASU) is being developed at the National Institute of Information and Communications Technology (NICT, Japan) as a part of the THz project^[14]. The THz project aims to develop THz technology for various applications concerning, for example, the telecommunications and atmospheric science. This paper focus on atmospheric science applications and more particularly on the Earth atmosphere remote sensing. However AMATERASU is also used for estimating the impact of the THz thermal atmospheric emission in the Earth energy budget and to study of other planetary atmospheres such as Venus or Mars planets. In case of atmospheric remote sensing, AMATERASU is used to define

instruments, quantify their capabilities and process the observations in order to retrieve geophysical parameters.

AMATERASU is based on the Microwave Observation Line Estimation and REtrieval (MOLIERE) code^[15] that has been developed at the Bordeaux Astronomical Observatory (France) to process the millimeter and submillimeter observations from the SubMillimeter Radiometer (SMR) onboard the Odin satellite^[16]. MOLIERE consists in a clear sky radiative transfer model for millimeter and submillimeter wavelengths region, a receiver simulator and an inversion code. This code can be applied to satellite, ground-based^[17] or downlooking balloon/airplane sounders. However the code can not be used when both uplooking and downlooking geometries should be considered together, and for limb geometry if the receiver is inside the atmosphere (e.g., balloon or airplane). For AMATERASU applications, the absorption coefficient module capability has been extended up to the near infrared region and a more general radiative transfer module has been developed to handle in one function the different geometries of the optical paths and any location for the receivers. A scattering module is also under development to take into account the effects of clouds in the radiative transfer. It is worthwhile to note that in the AMATERASU frequency range, the molecular rayleigh scattering can be neglected.

This paper aims to present AMATERASU focusing only on the modifications that has been added to MOLIERE. The receiver simulator and inversion codes remains unchanged and will not be described here. For the description of these modules, the reader should refer to the MOLIERE paper in the reference cited above. The scattering model is described in this issue^[18].

In section **2** we briefly present the necessary concepts to understand and use AMATERASU. A special focus is put on the absorption coefficient and the radiative transfer algorithms. The new computation of the radiative transfer is presented in section **3**. It

includes the calculation of the transmission and the radiance along the optical path as well as the computation of some geophysical parameters weighting functions. In section 4 we discuss the validation and the current applications of AMATERASU. We finally conclude in section 5 by giving the future evolutions of the model.

2 AMATERASU basis

2.1 Clear sky radiative transfer module

The clear sky radiative transfer module in AMATERASU calculates the integrated form of the non-scattered radiative transfer equation [19]:

$$I_\nu(s_r) = I_\nu(s_e) e^{-\int_{s_e}^{s_r} \alpha_\nu(s) ds} \quad (1)$$

$$+ \int_{s_e}^{s_r} B_\nu(T) \alpha_\nu(s) e^{-\int_s^{s_r} \alpha_\nu(s') ds'} ds \quad (2)$$

(Wm⁻²Hz⁻¹sr⁻¹).

This equation describes the processus of emission and absorption of the atmosphere at different positions s along a given optical path (s_e, s_r). $I_\nu(s_e)$ is the background radiance entering the optical path at the frequency ν and $I_\nu(s_r)$ is the outgoing radiance that is received by the sounder. The definition of the different physical parameters and constant used in this equation are given in the table 1. The background radiation is either the cosmologic radiation at 3 K or the Earth surface

emission. The scattering effect can be neglected as long as the clouds or aerosol are neglected (no particle of similar or larger size than the wavelength). The formulation of this equation assumes an atmosphere in the local thermodynamic equilibrium in order to set that the source function equals the absorption coefficient a_ν . This hypothesis is verified up to the upper mesosphere below the sub-millimeter wavelength range and to the mid-stratosphere for the IR region. When passing through the atmosphere, the line of sight is refracted and bended toward the surface. This effect is included and described in [15]. The details about the absorption coefficient are presented in the next section.

We define the opacity as $\tau_\nu(s, s_r) = \int_s^{s_r} \alpha_\nu(s) ds$ and the transmission $\eta_{s, s_r} = e^{-\tau_\nu(s, s_r)}$.

For the special case when the optical path goes through a medium with at a constant temperature T the equation 2 simply becomes:

$$I_\nu(s_r) = I_\nu(s_e) \eta_{s_e, s_r} + B_\nu(T)(1 - \eta_{s_e, s_r}) \quad (3)$$

The background radiation $I_\nu(s_e)$ is absorbed by a factor equal to the transmission η_{s_e, s_r} and a radiance $B_\nu(T)(1 - \eta_{s_e, s_r})$ is emitted by the medium. The outgoing radiance lies between I_{s_e} and $B(T)$. The net budget is a radiation absorption if $B_\nu(T) < I_\nu(s_e)$ or an emission otherwise.

For an optically thin medium, $\tau_{s_e, s_r} \approx 0$, the background radiation contribution is

Table 1 Definition and notation of the physical parameters and physical constants used in AMATERASU

Notations	Definitions	Values	Units SI
c	speed of light	$2.9979 \cdot 10^8$	m.s ⁻¹
h	Planck constant	$6.6261 \cdot 10^{-34}$	J.s
k_b	Boltzmann constant	$1.3807 \cdot 10^{-23}$	J.K ⁻¹
N	Avogadro number	$6.02 \cdot 10^{23}$	mol ⁻¹
R	ideal gaz constant ($k_b \times N$)	8.314	J.K ⁻¹
R_T	Earth radius	$6378 \cdot 10^3$	m
$B(T)$	Planck function		Wm ⁻² Hz ⁻¹ sr ⁻¹
$\alpha_\nu(s)$	absorption coefficient at the frequency ν		m ⁻¹
I_ν	radiance at the frequency ν		W.m ⁻² .Hz ⁻¹ .sr ⁻¹

approximated by $I_\nu(s_e)(1 - \tau_{s_e, sr})$ and the emitted radiance by $B_\nu(T) \tau_{s_e, sr}$. A small increase of the opacity (small enough to remain in the optically thin approximation) has a negligible effect on the background part but linearly increases the emitted radiance.

For an optically thick medium, $\tau_{s_e, sr} \gg 0$, the transmission is null and the outgoing radiation is simply $B(T)$. An small change in the opacity does not change the value of the outgoing radiation.

For intermediate cases, a small increase of the opacity will decrease the part of the background radiation and will increase the part of the emitted one. The outgoing radiation becomes closer to $B(T)$ and the difference $I_{sr} - I_{se}$ increases.

2.2 Absorption coefficient

2.2.1 The line by line model

The line by line model consists in computing along the optical path, the absorption coefficient, $a_\nu(s)$, for each spectroscopic transition and atmospheric constituent. The formulation of $a_\nu(s)$ is as follow:

$$\alpha(s, \nu) = \sum_p \sum_q \rho^p(s) I_{\nu_q}^q(T) \frac{\nu}{\nu_q} f^{p,q}(\nu, \nu_q) \quad (4)$$

(m^{-1})

where

- $\rho^p(s)$: density of the molecule p (m^{-3})
- ν_q : frequency of the transition q (Hz)
- I_{ν_q} : line strength of the transition q ($\text{Hz} \cdot \text{m}^2$)
- $f^{p,q}$: line shape for the molecule p and the transition q (Hz^{-1})

The transition frequency ν_q is slightly shifted by the pressure P . It is calculated as:

$$\nu_q = \nu_q^0 + \delta_\nu^q P \left(\frac{T_0}{T} \right)^{0.25+1.5n_a}$$

where ν_q^0 is the non shifted frequency transition, δ_ν^q is the pressure frequency shift parameter at the temperature T_0 and n_a is temperature dependence parameter.

The line strength is the probability for a molecule to pass from the upper energy level

to the lower energy level of the spectroscopic transition. It depends on the difference of population in the two levels and hence on the temperature when assuming the atmosphere in a thermal equilibrium. Given a line strength at a temperature T_0 , its value at the temperature T is given by [20]:

$$I_{\nu_q}(T) = I_{\nu_q}(T_0) \frac{e^{-E_q/k_b T}}{e^{-E_q/k_b T_0}} \left(\frac{1 - e^{-h\nu_q/k_b T}}{1 - e^{-h\nu_q/k_b T_0}} \right) \frac{Q^p(T_0)}{Q^p(T)} \quad (\text{Hz} \cdot \text{m}^2) \quad (5)$$

where E_q is the lowest energy of the two states of the transition q and Q^p is the partition function of the constituent p .

The line shape describes the broadening of the lines due to collision between molecules as well as an apparent line broadening due to the thermic random molecular velocity, i.e., a Doppler effect. The Doppler line shape is given by a Gaussian function f_d with a Half Width at Half Maximum (HWHM) $\Delta\nu_d$.

$$f_d(\nu, \nu_0) = \frac{1}{\Delta\nu_d} \left(\frac{\ln 2}{\pi} \right)^{\frac{1}{2}} e^{-\ln 2 \left(\frac{\nu - \nu_0}{\Delta\nu_d} \right)^2} \quad (\text{Hz}^{-1}) \quad (6)$$

$$\Delta\nu_d = \frac{\nu_q}{c} \left(\frac{2RT \ln 2}{M} \right)^{\frac{1}{2}} \quad (\text{Hz}) \quad (7)$$

where T is the temperature and M the molar mass.

The collisional line shape f_c is given by the Van Vleck and Weisskopf (VWV) profile [21]:

$$f_c(\nu, \nu_0) = \frac{1}{\pi} \frac{\nu}{\nu_q} \left(\frac{\Delta\nu_c}{\Delta\nu_c^2 + (\nu - \nu_q)^2} + \frac{\Delta\nu_c}{\Delta\nu_c^2 + (\nu + \nu_q)^2} \right) \quad (\text{Hz}^{-1}) \quad (8)$$

$$\Delta\nu_c = \gamma_{\text{air}} P (1 - \text{vmr}) \left(\frac{T_0}{T} \right)^{n_a} + \gamma_{\text{self}} P \text{vmr} \left(\frac{T_0}{T} \right)^{n_s} \quad (\text{Hz}) \quad (9)$$

where $\Delta\nu_c$ is the HWHM, γ_{air} and γ_{self} are the air and self broadening parameters at the temperature T_0 , P and T are the atmospheric pressure and temperature, and n_a and n_s are temperature dependence of the air and self broadening parameters.

The altitude dependence of the Doppler line width is only due to the temperature. Hence, the width remains on the same order of magnitude at all altitudes. On the other hand,

the collisional line width is proportional to the pressure and the width decreases exponentially with the altitude. At lower altitudes, the line width is dominated by the collisions effect and at upper altitudes, the Doppler broadening dominates. In between, both broadening mechanisms are taken into account and the corresponding line shape is the Voigt profile:

$$f_v(\nu, \nu_q) = \int_{-\infty}^{\infty} f_d(\nu, \nu_q) f_l(\nu - \nu', \nu_q) d\nu' \quad (\text{Hz}^{-1}). \quad (10)$$

Where f_l is the Lorentz profile that is an approximation of the VVW profile for small values of $\Delta\nu_c/\nu_q$:

$$f_l(\nu, \nu_q) = \frac{1}{\pi} \frac{\Delta\nu_c}{\Delta\nu_c^2 + (\nu - \nu_q)^2}.$$

The Voigt function has been multiplied by ν/ν_q in order to keep the same frequency dependence as in the VVW function. It exists several algorithms to perform the convolution and the one from Kuntz[22] is used in AMATERASU.

2.2.2 Continuum absorption

The line by line calculation is not enough to match the observed absorption coefficient value. First, the VVW lineshape fails to correctly represent the far wings of the line profile for high pressure. In the troposphere, the far wings of the H₂O and with a less extend CO₂, lead to large error in the calculated absorption coefficient.

Second, nonresonant absorption due to air

molecules (N₂, O₂, H₂O and CO₂) collisions leads to a continuum absorption that is important in the lower and mid troposphere. Theoretical formulation of the collision induced continuum has been calculated[23]-[25].

In AMATERASU the value of the far wings of the line profile are set to zero from a distance from the line center set by the user (the default value is 25 cm⁻¹). The MT_CKD model[26] is used to account for the O₂, N₂, CO₂ and H₂O continua. It covers the full IR region including the microwave region. However the accuracy of the water vapor continuum is uncertain in the sub-millimeter and THz waves domain. In the future, we will include the water vapor continuum parametrization that is currently being measured in NICT in this frequency domain[14]. The other absorption continuum models that was in MOLIERE are also included[27][28]. However these models are valid only up to more or less 1 THz. For a simulation at frequencies below 400 GHz, the Liebe model should be used for dry air and water vapor continua. The liebe model[27] implementation also includes its own line by line model taking into account the most important H₂O and O₂ lines below 1 THz. For planetary atmosphere studies, the CO₂-CO₂ continuum absorption model from[25] has also been implemented.

2.3 Spectroscopic databases

AMATERASU reads the spectroscopic

Table 2 Description of the main parameters in the MOLIERE lines catalog

Notations	Definitions	Position (format ¹)
<i>SPEISO</i>	molecular tag ²	1-3 (i3)
<i>FRE</i>	Frequency of the transition [MHz]	4-16 (f13.4)
<i>FSH</i>	Frequency shift parameter at 296 K [MHz/hPa]	24-32 (f8.3)
<i>STG</i>	Log10 of the line strength at 300 K [MHz·nm ²]	33-40 (f8.4)
<i>ELO</i>	Energy of the lowest transition level [cm ⁻¹]	41-50 (f10.4)
<i>AGA</i>	air-collisional broadening parameter [MHz/hPa]	51-55 (f5.2)
<i>SGA</i>	self-collisional broadening parameter [MHz/hPa]	56-60 (f5.2)
<i>N</i>	air broadening temperature dependence parameter [-]	61-64 (f4.2)
<i>NS</i>	self broadening temperature dependence parameter [-]	65-68 (f4.2)

¹ Fortran language format notation

² use HITRAN convention (e.g. 12 for H₂¹⁸O)

Table 3 HITRAN parameters to AMATERASU parameters conversion

Parameter	HITRAN unit	conversion formula
<i>FRE</i>	cm ⁻¹	HITRAN_VALUE × <i>c</i> × 10 ⁻⁴
<i>FSH</i>	cm ⁻¹ /atm ⁻¹ at 296 K	HITRAN_VALUE × <i>c</i> × 10 ⁻⁴ /760.
<i>STG</i>	cm ⁻¹ /cm ² at 296 K*	log ₁₀ (HITRAN_VALUE × <i>c</i> × 10 ¹² /r _{iso})
<i>AGA</i>	cm ⁻¹ /atm ⁻¹	HITRAN_VALUE × <i>c</i> × 10 ⁻⁴ /760.

* line strength must be computed at 300 K (Eq 5)

parameters from the same catalog as MOLIERE. The different fields are given in Table 2. The HITRAN spectroscopic database[29] is used to create the lines file. The conversion rules between one catalog to the other are given in Table 3. The database from the Jet Propulsion Laboratory[20] can also be used but the spectroscopic catalog does not provide the pressure broadening parameters.

3 Computation of the radiative transfer equation and derivation of the weightig functions

3.1 Transmission and outgoing Radiance

The radiative transfer equation 2 is discretized by dividing the atmosphere in layers with constant temperature. The thickness of each layer is defined so that the optical path traverses the same distance in each layer. The discretized transmission between the layer *i* up to the layer *j* (not included) is noted $\eta [i : j]$. The indexes of the first and last layer are 1 and *n*, respectively. The receiver is indicated with the index *n* + 1. Neglecting the frequency dependence in the notation, the radiative transfer equation becomes:

$$I[n + 1] = I[0] \times \eta [1 : n + 1] + \sum_{i=1}^{n-1} \{B[i] \times (\eta [i + 1 : n + 1] - \eta [i : n + 1])\} + B[n] \times (1 - \eta [n : n + 1]) \quad (11)$$

given the relation $\eta [i : j] = \prod_{k=i}^{j-1} \eta [k]$ and the radiance emitted by the layer *i* that reaches the receiver is:

$$I[i] = B_i (1 - \eta [i : i + 1]) \eta [i + 1 : n + 1]. \quad (12)$$

In Equation 12, the term $B_i (1 - \eta [i, i + 1])$ is the radiance emitted by the layer *i* (Eq. 3) and $\eta [i + 1, n + 1]$ is the transmission (i.e., level of absorption) from the layer *i* to the receiver.

As already pointed out in the previous section, for an optically thick atmosphere, given that $\eta [1 : n + 1] \approx 0$, and $\sum_i^n \eta [i + 1 : n + 1] - \eta [i : n + 1] = 1 - \eta [1 : n + 1] \approx 1$, the outgoing radiance $I [n + 1]$ is a weighted average of the Planck radiance B_i of each layer *i*. When the radiance is expressed in brightness temperature, the outgoing radiance is the mean temperature of the layers that significantly contribute to it (see Fig. 1). The shape of the contribution function is related to the altitude dependence of the atmospheric opacity.

3.2 The VMR Weighting functions

The derivation of the discretized radiative transfer equation with respect to the Volume Mixing Ratio (VMR) $x[l]$ in the layer *l* of a given atmospheric constituent is given by:

$$K[l] = \frac{\partial I[n + 1]}{\partial x[l]} = -\bar{\alpha}[l] \times \Delta[l] \times (I[0] \times \eta [1 : n + 1] + \sum_{i=1}^{l-1} B[i] \times (\eta [i + 1 : n + 1] - \eta [i : n + 1]) + -B[l] \times \eta [l : n + 1],)$$

where $\Delta [l]$ is the optical path length in the layer *l*, $\bar{\alpha} [l] = \frac{\partial \alpha [l]}{\partial x [l]} [l] = \rho [l] k [l]$ and $\rho [l]$ is the atmospheric density and $k [l]$ the absorption cross-section in the layer *l*.

To derive the weighting functions expression, we use:

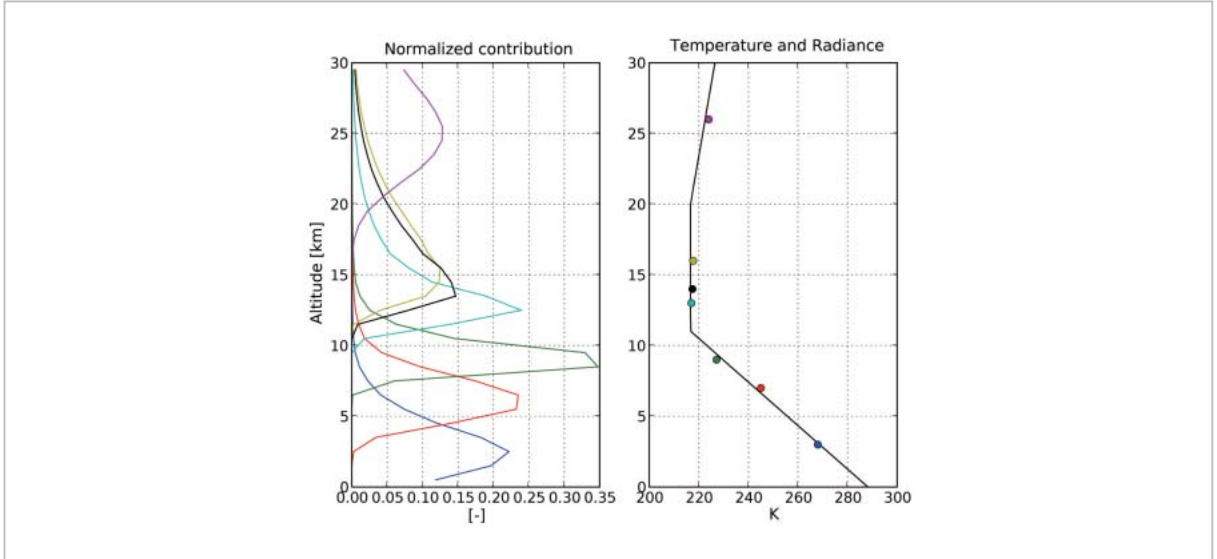


Fig. 1 Left panel: The normalized contribution functions (Eq. 12) for a nadir observation are shown at 7 frequencies between 0.1 to 5 THz. The atmospheric opacity is 4 for the lowest contribution function and 30×10^4 for the upper function. Right panel: the atmospheric temperature (black curve) is shown together with the brightness temperature (circle) corresponding to the same opacity levels as used in the left panel. The dots indicate both the maximum altitude of the contribution function and the brightness temperature of the outgoing radiation

$$\frac{\partial \eta[j : n + 1]}{\partial x[l]} = \begin{cases} -\bar{\alpha}[l] \times \Delta[l] \eta[j : n + 1], & \text{if } l \in [j, n] \\ 0, & \text{if } l \neq [j, n] \end{cases}$$

Noting the common terms in Equation 12, it is possible to implement a fast algorithm to calculate simultaneously the weighting functions and the radiance.

3.3 The Temperature weighting functions

As for the VMR weighting functions, it is possible to derive the discretized form of the radiative transfer equation with respect to the temperature of the layer l :

$$\begin{aligned} K^T[l] &= \frac{\partial I[n + 1]}{\partial T[l]} \\ &= -\frac{\partial \alpha[l]}{\partial T[l]} \times \Delta[l] \times (\\ &+ I[0] \times \eta[1 : n + 1] \\ &+ \sum_{i=1}^{l-1} B[i] \times (\eta[i + 1 : n + 1] - \eta[i : n + 1]) \\ &+ -B_f[l] \times \eta_f[l : n + 1] \\ &) \\ &+ \frac{\partial B_f[l]}{\partial T[l]} \times (\eta[i + 1 : n + 1] - \eta[i : n + 1]) \end{aligned}$$

The term $\frac{\partial \alpha[l]}{\partial T[l]}$ is calculated by a perturba-

tion method.

3.4 Source function weighting functions

Let's replace in Equation 12 the Planck function $B[i]$, by the source function:

$$S[i] = \beta[i] \times B[i] + \varepsilon[i].$$

The derivative of Equation 12 with respect to $\beta[i]$ is:

$$\begin{aligned} K^s[l] &= \frac{\partial I[n + 1]}{\partial \beta[l]} \\ &= B[l] \times (\eta[l + 1 : n + 1] - \eta[l : n + 1]). \end{aligned}$$

It is interesting to note that $K^s[l]$ is $I[l]$ (Eq. 12), the contribution of the layer l to the outgoing radiance $I[n + 1]$.

The derivative of Equation 12 with respect to $\varepsilon[l]$ is:

$$K^e[l] = \eta[l + 1 : n + 1] - \eta[l : n + 1]$$

4 Model validation and Current applications

The validation of the model is performed

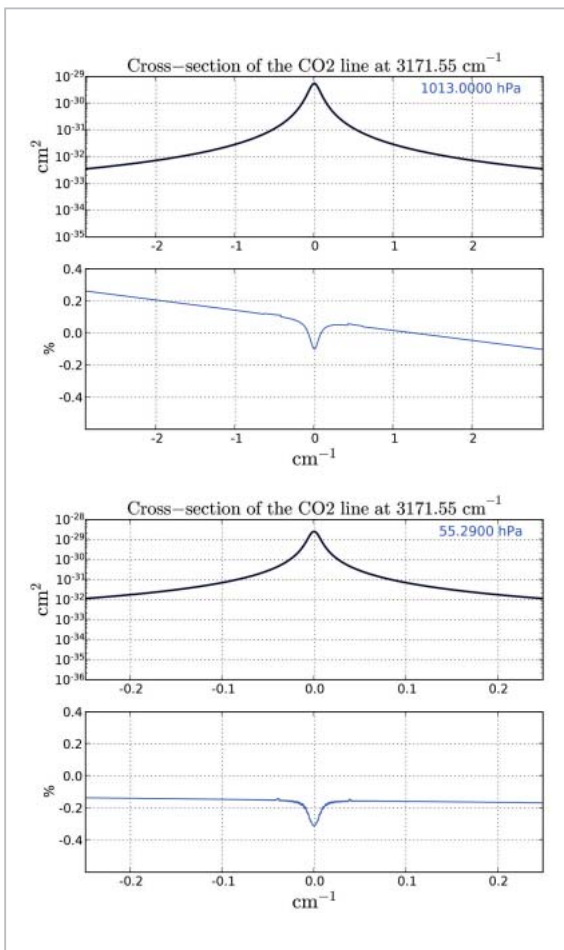


Fig.2 Upper panel: Cross section of the CO₂ line at 3171.5 cm⁻¹ calculated at 1013.25 hPa using MIRART (thick blue line) and AMATERASU (dash black line). The bottom panel shows the relative difference between both calculation. Lower panel: Same as the left panel but for a pressure of 50 hPa

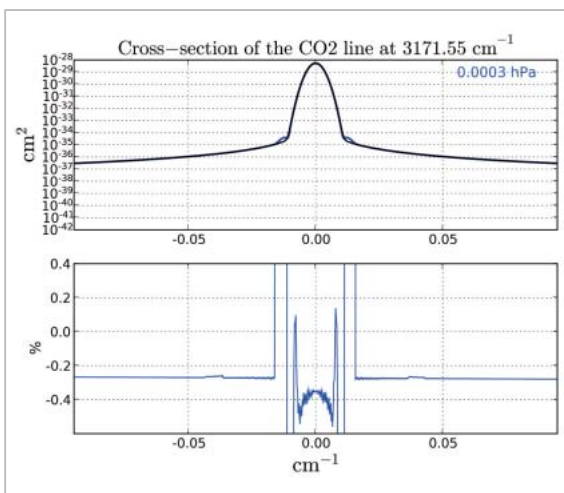


Fig.3 Same as Fig. 2 but for a pressure of 10⁻⁴ hPa

in 2 steps. In a first step, the code is compared to other algorithms in order to verify the correctness of the implementation and the numerical accuracy. In this step a special care is put on the absorption coefficient and the radiative transfer computations. The code MOLIERE has already been compared with several models in the millimeter and sub-millimeter regions[30]. After each change, the new version of AMATERASU has been compared with MOLIERE when it is possible. In particular we checked that the new radiative transfer calculation agrees with MOLIERE for up-looking, down-looking and limb-looking geometries with differences less than 1 %.

In the second step the model is validated against real measurements in order to check the validity of the algorithm hypothesis.

We briefly present in the next section a comparison of the line by line calculation performed by AMATERASU with the code MIRART[31]. The comparison has been realized in the framework of the use of AMATERASU absorption coefficient to retrieve CO₂ concentration from LIDAR observations. The concentration measured by the LIDAR system agrees with in situ measurements.

We also present the analysis to retrieve geophysical parameters from the Balloon Far InfraRed SpecTrometers (FIRST) observations. They are the first observations of the atmospheric outgoing radiance spectrum in the full IR spectral range (up to 2000 cm⁻¹) including the THz region[13].

Currently, the code is also used in other studies that are not presented in this paper. Let's mention the retrieval of stratospheric and mesospheric HO₂ distribution from the Sub-Millimeter Radiometer on board the Odin satellite[9][32] and the studies to improve the processing chain of the Super-conductive Sub-Millimeter Limb Emission Sounder (SMILES) that will be launched in 2009 in the Japanese Experimental Module (JEM) of the International Space Station[33]. AMATERASU is also used to study the Venus and Mars atmospheres.

4.1 Comparison of CO₂ cross-section with the MIRART model

The computations of the CO₂ cross-section by AMATERASU and MIRART have been compared at 3 different pressure levels 1013.25, 50, and 10⁻⁴ hPa. We can consider that the line is broadened by collisions at 1013.25 hPa, by Doppler effect at 10⁻⁴ hPa, and by both effects at 50 hPa. Beside the implementation itself, the differences are from the Voigt algorithm, the partition functions and the isotopic ratio. In this calculation MIRART does not include self-collisional broadening effect but, we verified with AMATERASU that it has a neglectible impact on the results. Only one line is used at 3371.5 cm⁻¹ that is extracted from the HITRAN catalog. While the MIRART code uses directly this catalog, the HITRAN parameters have to be converted in the AMATERASU lines file format and units. The comparison between both codes also validates the conversion procedure from the HITRAN to the AMATERASU lines file.

For the 2 highest pressure levels, a good agreement is found since the differences between the models is below 0.5 %. For the pressure level at 10⁻⁴ hPa, within 0.01 cm⁻¹ the line shape is the Doppler Gaussian function. In this region, the agreement between both models is very good (below 0.5 %). Outside this range, the lineshape follows the collisional line shape. In the transition domain between the two regimes, the MIRART shows two symmetric lobes that are not reproduced by AMATERASU. However the cross section value is very low and this effect can be neglected.

Hence, we can conclude that the comparison indicates a good agreement between the line by line algorithms of AMATERASU and MIRART.

4.2 Balloon FIRST observations

The FIRST instrument is a Michelson interferometer capable of sensing the spectral region between 100 to 1000 cm⁻¹ with a resolution of 0.625 cm⁻¹ (unapodized). The instrument flew on a high altitude balloon recording

for the first time the nadir Earth outgoing Long wave Radiation from almost the full IR region. Using AMATERASU we want to demonstrate with this instrument the benefits of adding the THz region with the mid-IR region for retrieving the upper tropospheric humidity from space.

AMATERASU has been configured to simulate the FIRST instrument observations. The theoretical unapodized instrumental line-shape has been used (Eq. 13) and it has been modeled over a spectral range of 12 cm⁻¹ and a resolution of 0.1 cm⁻¹.

$$f(\nu) = \frac{\sin(\pi\nu/d\nu)}{(\pi\nu/d\nu)}, \quad (13)$$

with $d\nu = 0.625$ cm⁻¹.

A comparison between the FIRST spec-

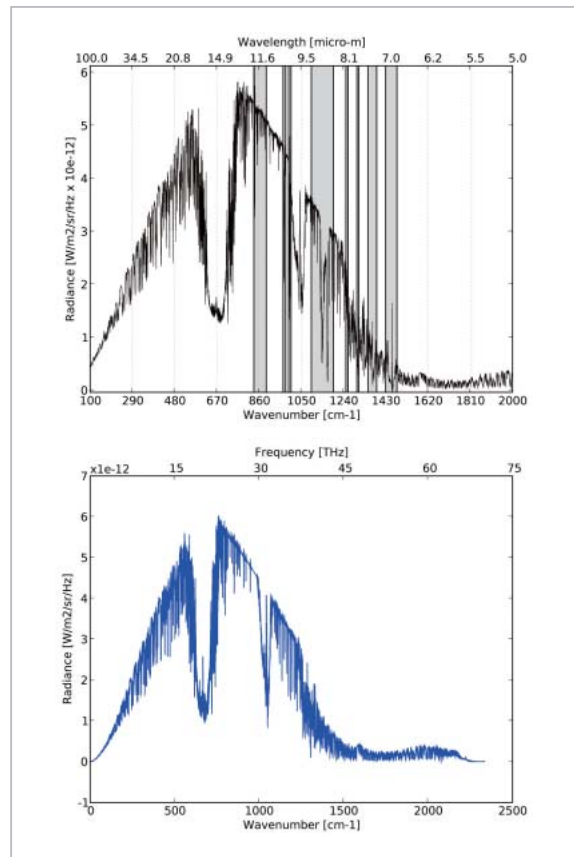


Fig.4 Upper panel: Mean spectrum observed by FIRST between 7:11 pm to 8:50 on June 7, 2005. Lower Panel: Simulated outgoing long wave radiance. The radiances have been computed using a mid-latitude climatology and the theoretical instrument line shape

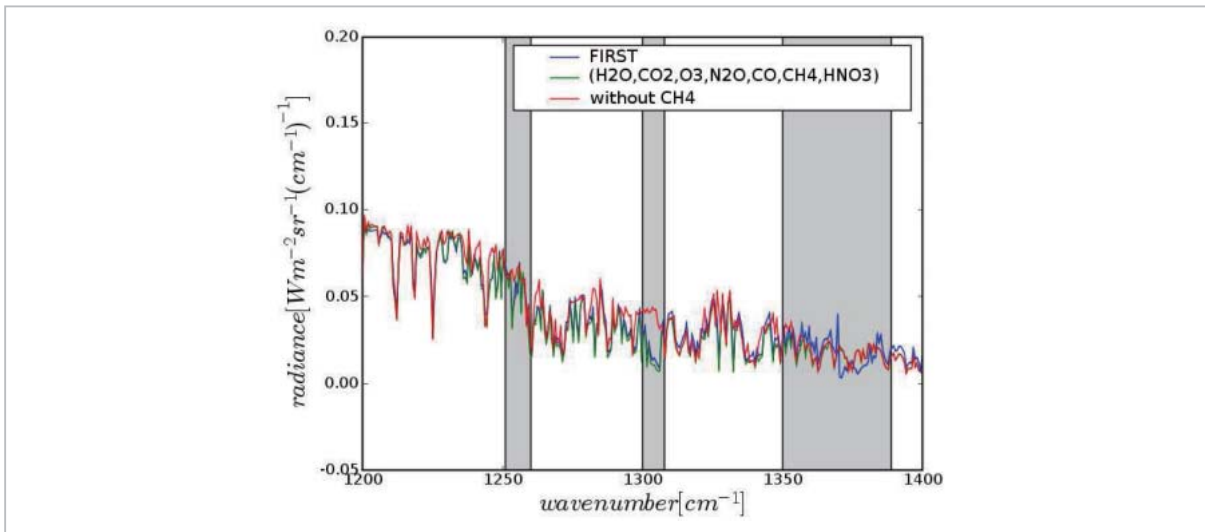


Fig.5 Mean FIRST spectrum (blue line) together with two AMATERASU calculations in the infrared CH_4 absorption band. The first calculation includes the main absorbing lines (green line) and in the second calculation (red line), the CH_4 lines have been removed. The radiances have been computed using a mid-latitude climatology and the theoretical instrument line shape

trum and a AMATERASU simulation is shown in Figure 4. In parallel, a study is carried out in order to retrieve tropospheric methane (CH_4). Figure 5 shows the FIRST spectrum within the selected frequency range. It is also shown two AMATERASU calculations with and without CH_4 lines.

Taking into account that the atmospheric description comes a climatology, the FIRST observations and the full simulation with AMATERASU can be considered in a good agreement. The simulation without the CH_4 spectroscopic lines shows the locations of the CH_4 lines that will be used to retrieve the CH_4 concentration. The other lines are from H_2O and N_2O .

5 Conclusion

We have presented the model AMATERASU for the analysis and the simulation of THz radiation. The current status of the model

already allows to use it in several studies. However it has to be improved.

The scattering module that is currently developed will be fully integrated. The possibility to take into account horizontal inhomogeneities along the optical path will also be included.

The far wings of the line shape has to be improved by using other profile than the VVW profile. The interferences between close CO_2 lines in the $15 \mu\text{m}$ window (line mixing) has to be taken into account. In parallel, the algorithms must be fully validated following the methodology described in this paper.

Acknowledgments

We would like to thank Dr Marty Mlynczak and Dr David Johnson (NASA Langley Research Center) for having provided the FIRST data.

References

- 1 J. E. Harries, J. E. Russell, and co authors, "The Geostationary Earth Radiation Budget (GERB) experiment", *Bull. Amer. Met. Soc.*, 86:945-960, 2005.
- 2 SPARC. Assessment of upper tropospheric and lower stratospheric water vapour, 2000.
- 3 H. K. Roscoe, "A review of stratospheric H₂O and NO₂", *Advances in Space Research*, 34(8):1747-1754, 2004.
- 4 IPCC. Climate change 2001: The scientific basis, 2001.
- 5 M. O. Andreae, Artaxo P., Fischer H., Freitas S. R., Grégoire J.-M., Hansel A., Hoor P., Kormann R., Krejci R., Lange L., Lelieveld J., Lindinger W., Longo K., Peters W., de Reus M., Scheeren B., Silva Dias M. A. F., Ström J., van Velthoven P. F. J., and Williams J., "Transport of biomass burning smoke to the upper troposphere by deep convection in the equatorial region", *Geophys. Res. Lett.*, 28:951-954, Mar. 2001.
- 6 B. N. Duncan, S. E. Strahan, Y. Yoshida, S. D. Steenrod, and N. Livesey, "Model study of the cross-tropopause transport of biomass burning pollution", *Atmos. Chem. Phys.*, 7:3713-3736, 2007.
- 7 A. Stohl, Forster C., Eckhardt S., Spichtinger N., Huntrieser H., J. Heland, Schlager H., Wilhelm S., Arnold F., and Cooper O., "A backward modeling study of intercontinental pollution transport using aircraft measurements", *J. Geophys. Res.*, 108(D12), 2003.
- 8 P. W. Rosenkranz, "Retrieval of temperature and moisture profiles from AMSU-A and AMSU-B measurements", 39:2429-2435, 2001.
- 9 D. P. Murtagh, U. Frisk, F. Merino, M. Ridal, A. Jonsson, J. Stegman, G. Witt, P. Eriksson, C. Jiménez, G. Mégie, J. de La Noë, P. Ricaud, P. Baron, J. R. Pardo, A. Hauchecorne, E. J. Llewellyn, D. A. Degenstein, R. L. Gattinger, N. D. Lloyd, W. F. J. Evans, I. C. McDade, C. S. Haley, C. Sioris, C. von Savigny, B. H. Solheim, J. C. McConnell, K. Strong, E. H. Richardson, G. W. Leppelmeier, E. Kyrölä, H. Auvinen, and L. Oikarinen, "An overview of the Odin atmospheric mission", *Can. J. Phys.*, 80(4):309-318, 2002.
- 10 J. W. Waters, L. Froidevaux, R. S. Harwood, R. F. Jarnot, H. M. Pickett, W. G. Read, P. H. Siegel, R. E. Cofield, M. J. Filipiak, D. A. Flower, J. R. Holden, G. K. Lau, N. J. Livesey, G. L. Manney, H. C. Pumphrey, M. L. Santee, D. L. Wu, D. T. Cuddy, R. R. Lay, M. S. Loo, V. S. Perun, M. J. Schwartz, P. C. Stek, R. P. Thurstans, M. A. Boyles, S. Chandra, M. C. Chavez, G-S. Chen, B. V. Chudasama, R. Dodge, R. A. Fuller, M. A. Girard, J. H. Jiang, Y. Jiang, B. W. Knosp, R. C. LaBelle, K. A. Lee, D. Miller, J. E. Oswald, N. C. Patel, D. M. Pukala, O. Quintero, D. M. Scaff, W. V. Snyder, M. C. Tope, P. A. Wagner, and M. J. Walc.
- 11 A. Chedin, M. T. Chahine, and N. A. Scott, editors, "High Spectral Resolution Infrared Remote Sensing for the Earth's Weather and Climate Studies", NATO ASI Series, Vol.19, Springer, 1993.
- 12 H. Fischer and H. Oelhaf. "Remote sensing of vertical profiles of atmospheric trace constituents with MIPAS limb – emission spectrometers". 35:2787-2796, 1996.
- 13 Mlynchak M. G., Johnson D. G., Latvakosky H., Watson M., Kratz D. P., Traub W. A., Bingham G. E., Wellard S. J., Hyde C. R., and X. Liu, "First light from the far-infrared spectroscopy of the troposphere (first) instrument", *Geophysical Research Letters*, 33:L07704, 2006.
- 14 I. Hosako, N. Sekine, M. Patrashin, S. Saito, K. Fukunaga, Y. Kasai, P. Baron, T. Seta, J. Mendrok, S. Ochiai, and H. Yasuda, "At the dawn of a new era in terahertz technology", vol.95 (8), pp.1611-1623, 2007.

-
- 15 J. Urban, P. Baron, N. Lauté, N. Schneider, K. Dassas, P. Ricaud, and J. De La Noë, "Moliere (v5): a versatile forward – and inversion model for the millimeter and sub-millimeter wavelength range", *JQSRT*, 83:529-554, 2004.
 - 16 P. Baron, *Developpement et validation du code MOLIERE: Chaîne de traitement des mesures micro-ondes du satellite Odin*, PhD thesis, Université Bordeaux I, Jun. 1999.
 - 17 P. Ricaud, P. Baron, and J. de La Noë, "Quality assessment of ground-based microwave measurements of chlorine monoxide, ozone, and nitrogen dioxide from the ndsc radiometer at the plateau de bure", *Annales Geophysicae*, 22:1903-1915, 2004.
 - 18 J. Mendrok and P. Baron, "The AMATERASU Scattering Module", Review of the National Institute of Information and Communications Technology, in this issue, 2008.
 - 19 S. Chandrasekhar. *Radiative Transfer*. Dover Publications, Inc., New-York, 1960.
 - 20 R. L. Poynter and H. Pickett, "Submillimeter, millimeter, and microwave spectral line catalog", *Applied Optics*, 23:2235-2240, 1985.
 - 21 J. H. Van Vleck and V. F. Weisskopf, "On the shape of collision-broadened lines", *Review of modern physics*, 17(2 and 3):227-236, 1945.
 - 22 M. Kuntz, "A new implementation of the humlicek algorithm for the calculation of the voigt profile function", *J. Quant. Spectrosc. Radiat. Transfer*, 57(6), 1997.
 - 23 A. Borysow and L. Frommhold, "collision induced rototranslational absorption spectra of n₂-n₂ pairs for temperatures from 50 to 300 K", *Astrophysical Journal*, 311, 1986.
<http://www.astro.ku.dk/aborysow/programs/index.html>.
 - 24 J. Boissoles, C. Boulet, R. H. Tipping, A. Brown, and Q. Ma, "Theoretical calculation of the translation-rotation collision-induced absorption in N₂-N₂, O₂-O₂, and N₂-O₂ pairs", *J. Quant. Spectrosc. Radiat. Transfer*, 82:505-516, 2003.
 - 25 M. Gruszka and A. Borysow, "Roto-translational collision-induced absorption of CO₂ for the atmosphere of Venus at frequencies from 0 to 250 cm⁻¹ and at temperature from 200 K to 800 K", *Icarus*, 129:172-177, 1997.
 - 26 E. J. Mlawer, S. C. Clough, and D. C. Tobin. MT-CKD model, version 1.2, from <http://www.rtweb.aer.com/main.html>. 2004.
 - 27 H. J. Liebe, "Propagation modeling of moist air and suspended. water/ice particles at frequencies below. 1000 ghz", In *Proceedings of the AGARD 52nd specialists meeting electromagnetic propagation panel*.
 - 28 J. R. Pardo, E. Serabyn, M. C. Wiedner, and J. Cernicharo, "Measured telluric continuum-like opacity beyond 1 THz", *J. Quant. Spectrosc. Radiat. Transfer*, 2005.
 - 29 L. S. Rothman, D. Jacquemart, A. Barbe, D. C. Benner, M. Birk, L. R. Brown, M. R. Carleer, Jr. C. Chackerian, K. Chance, L. Coudert, V. Dana, V. M. Devi J. M. Flaud R. R. Gamache, A. Goldman, J. M. Hartmann, K. W. Jucks, A. G. Maki, J. Y. Mandin, S. T. Massie, J. Orphal, A. Perrin, C. P. Rinsland, M. A. H. Smith, J. Tennyson, R. N. Tolchenov, R. A. Toth, J. Vander Auwera, P. Varanasi, and G. Wagner, "The HITRAN 2004 molecular spectroscopic database", *JQSRT*, 96:1747-1754, 2005.
 - 30 C. Melsheimer, C. Verdes, S. Bühler, C. Emde, P. Eriksson, S. Ichizawa, V. O. John, Y. Kasai, G. Kopp, N. Koulev, T. Kuhn, O. Lemke, S. Ochiai, F. Schreier, T. R. Sreerekha, C. Takahashi, S. Tsujimaru, and J. Urban, "Intercomparison of general purpose clear-sky atmospheric radiative transfer models for the millimeter and sub-millimeter spectral range", *Radio Science*, 40:RS1007, 2005.

- 31 F. Schreier and U. Böttger, "MIRART, a line-by-line code for infrared atmospheric radiation computations incl. derivatives", *Atmos. & Oceanic Optics*, 16:262-268, 2003.
- 32 P. Baron, Y. Kasai, D. P. Murtagh, J. Urban, P. Erickson, and M. Olberg, "HO₂ measurement in the stratosphere and the mesosphere from the sub-millimeter limb sounder Odin/SMR", *Advances in Geosciences 2006 (Atmospheric Science)*, 06, 2007.
- 33 M. Shiotani, H. Masuko, and the SMILES Science Team and the SMILES Mission Team, "JEM/SMILES mission plan", NASDA Rep. Version 2.1, National Space Development Agency (NASDA), Communications Research Laboratory (CRL), Koganei, Tokyo, 184-8795, Japan, Nov.15 2002. <http://smiles.tksc.nasda.go.jp/indexe.shtml>.

Philippe Baron, Ph.D.

*Expert Researcher, Environment Sensing and Network Group, Applied Electromagnetic Research Center
Development of Forward and Retrieval Models for Atmospheric Remote Sensing*



Jana Mendrok, Ph.D.

*Expert Researcher, Environment Sensing and Network Group, Applied Electromagnetic Research Center
Radiative Transfer Modeling and Cloud Remote Sensing*

KASAI Yasuko, Ph.D.

*Senior Researcher, Environment Sensing and Network Group, Applied Electromagnetic Research Center
Terahertz Remote Sensing*

OCHIAI Satoshi

*Senior Researcher, Environment Sensing and Network Group, Applied Electromagnetic Research Center
Micro Wave Remote Sensing*

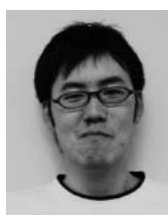
SETA Takamasa

*Expert Researcher, Advanced Communications Technology Group, New Generation Network Research Center
Physical Chemistry, Spectroscopy, Reaction Kinetics, Atmospheric Chemistry*



SAGI Kazutoshi

*Bachelor, Earth Life Environmental Science Faculty, Science Department, Ibaraki University
Earth and Planetary Science*



SUZUKI Kodai

*Bachelor, Environmental science Faculty, Education Department, Tokyo Gakugei University
Earth and Planetary Science*



SAGAWA Hideo, Ph.D.

*Max Planck Institute for Solar System Research, Germany
Remote Sensing of the Planetary Atmosphere*

Joachim urban, Ph.D.

*Research Scientist, Chalmers University
Earth and Planetary Science*